DELTA JOURNAL OF SCIENCE 2006, 30, 117 - 132

RADIOACTIVITY AND MINERALOGICAL INVESTIGATIONS ON YOUNGER GRANITES OF GABAL SHEIKH EL-ARAB AREA, SOUTHERN SINAI, EGYPT

ABDEL MONEM M. OSMAN*, IBRAHIM E. AASSY**, ALI A. EL MOWAFY**, SALAH S. EL BALAKSSY** AND OSAMA R. SALLAM**

*Geology Department, Faculty of Science, Ain Shams University, Cairo, Egypt.

**Nuclear Materials Authority, P.O. Box; 530El-Maadi, Cairo, Egypt.

(Received: 4 Jaune, 2006)

ABSTRACT

The younger granites of the studied area vary in composition from monzogranite, syenogranite to alkali feldspar granite. They exhibit silicification, kaolinitization and ferrugination as a result of the post–magmatic hydrothermal alteration. The monzogranite is traversed by quartz veins and shear zone, while the syenogranite invaded by pegmatitic bodies. Two radioactive anomalies were recorded in the shear zone, as well as, in pegmatites. Petrographic investigation, XRD analyses and ESEM examination show that, pegmatites contain apatite, bastnasite, betafite, brannerite, cassiterite, columbite, fluorite, goethite, lanarkite, lepidocrocite, malachite, parisite, pisckite, polycrase, thalenite, thorite, xenotime, yttrocrasite, zircon and metamict zircon. Shear zone displays bismite, fluorite, goethite, hematite, ilmenite, lanarkite, lepidocrocite, malachite, phlogopite, thorite and uranothorite minerals.Quartz veins exhibit goethite and hematite minerals. The identified minerals reflect the importance of the pegmatites and the shear zone for the REE.

INTRODUCTION

The Egyptian granites are classified into two main types, the older (calc-alkaline) granites and the younger (late tectonic to post tectonic) granites (Akaad and El-Ramly, 1960; El-Ramly, 1972; Stern *et al.*, 1984). The granitic rocks in southern Sinai which represent extremity the northwestern part of the exposed crystalline rocks of the Arabian–Nubian Shield, and hence they show an evolution trend from the older calc-alkaline subduction-related granites (GI) to younger alkaline (post-orogenic) granites (GII) and finally the peralkaline granites (anorogenic) granites (GIII) (Hussein et al., 1982). Alkali granites seem to be more widespread in Sinai than in any other part of the Shield, where they form about 20% of the granites in Sinai (Bentor, 1985), and were intruded during the time span between 560+10 and 580+6 Ma (Halpern, 1980).

Gabal Sheikh El-Arab area lies at the southern part of Sinai Peninsula. It is bounded by lat. 28° 20 and 28° 30 N and long. 33° 55 and 34° 05 E (Fig. 1). The country rocks are mainly metasediments, older granites, Dokhan volcanics, Hammamat sediments, Katherine ring dyke, Katherine volcanics, younger granites and quartz syenite. This work will deal only with the younger granites, which traversed by pegmatites, shear zone and quartz veins.The younger granites vary in composition from monzogranite through syenogranite to alkali feldspar granite. They display characteristic features as cavernous, exfoliated and highly jointed. The silicification, kaolinitization, ferrugination and the dendrite manganese oxides are the main fracture filling in monzogranite. It represents the post–magmatic hydrothermal alteration features. The unzoned pegmatite bodies (0.20 x 0.30 m to 1.00 x 1.5 m in dimensions) hosted in syenogranite, occur either as oval-shape or as veins and show high radioactivity especially at W. Rutig. The shear zone vary from 0.5 to 2.5 m in width, trending N 55° W with 62° dip and traversed monzogranite at W. El-Ruseis. It was affected by hydrothermal solution and exhibit several minerals such as, malachite, iron oxides, lead, bismuth, uranium and thorium. The malachite

ISSN 1012 – 5965

and iron oxides occur as filling fissures and cracks, or as scattered. Ibrahim (1996) indicated that, the shear zones at W. El-Ruseis exhibit malachite, ilmenite, hematite, titanite, phlogopite and some radioactive minerals. The quartz veins (about 5 to 25 cm thickness) trending E-W with 68°-75° dip crosscut monzogranite at W. El-Ruseis and contain iron oxides mineralization.

SAMPLING AND METHODOLOGY

Thirty four samples were collected from the study area. The first twenty four samples from the younger granites, four samples from pegmatites, three altered rock samples from shear zone and three samples from quartz veins. Thin sections represent the examined rocks were prepared for petrographic studies. The trace elements of 20 samples from the different rocks under consideration were measured using X-ray fluorescence and atomic absorption. The major oxides were determined using the wet chemical techniques. The radiometric analyses using Gamma-ray spectrometry multichannel analyzer were carried out on some selected samples. In addition, microscopical investigations for grains, X-ray diffraction analyses (XRD) and Environmental Scanning Electron Microscope (ESEM) examination using Philips apparatus model XL, 30; Energy Dispersive X-ray (EDX) and Back-Scattered Electron (BSE) Image were applied for mineralogical investigations. All analyses were done in the Central Laboratories of the Nuclear Materials Authority (NMA).

PETROGRAPHY

The modal composition of the studied younger granites (22 samples) is listed in table (1). The obtained data are plotted on the QAP ternary diagram (Fig. 2) after Streckeisen (1976). It is clear that, the studied younger granites range in composition from monzogranite through syenogranite to alkali feldspar granite. Opaques, sphene, fluorite, zircon and apatite are the main accessories in the studied younger granites, while, kaolinite, sericite, chlorite and iron oxides represent the secondary minerals. The petrographic investigations of pegmatites revealed that, fluorite occurs in association with thorite in (Figs. 3a & b). The shear zone shows that, uranothorite and iron oxides are of fissure fillings (Fig. 3c). On the other hand, in quartz veins the interstitial spaces between quartz crystals are filled with iron oxides (Fig.3d).

GEOCHEMISTHY

The major oxides and some trace elements of the examined rocks are given in tables(2 and 3). They revealed that, the younger granites show a normal content of major oxides and trace elements. R1-R2 discrimination diagram Fig.(4) of De La Roche et al. (1980) indicates that, the studied younger granites display alkali feldspar granite, syenogranite and monzogranite fields. On the other hand, the pegmatites attain high concentration of Zr, Y, Nb, Rb and Ba, shear zone shows high concentration of Fe_2O_3, Cu and Ba, whereas, quartz veins exhibit high concentration of Fe_2O_3.

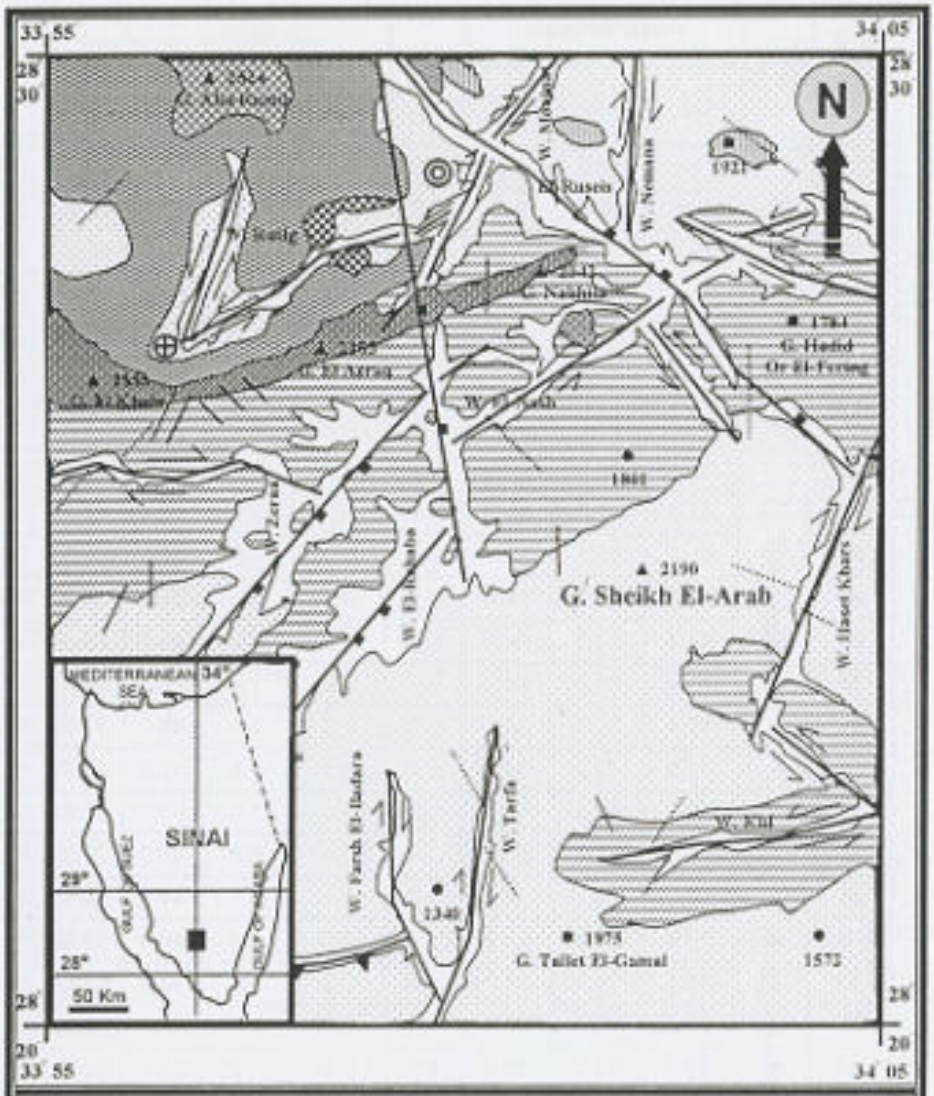

Fig. (1): Geological map of Gabal Sheikh El-Arab area.

Youngest

- Dykes
- Quartz Syenite
- Younger Granites
- Katherine Volcanics
- Katherine Ring Dyke
- Hammamat Sediments
- Dokhan Volcanics
- Older Granites
- Metasediments

Oldest

- Normal fault (Up / Down)
- Strike slip fault
- Thrust fault
- joint
- Geological contact
- Radioactive pegmatite anomaly
- Radioactive shear zone anomaly
- 2190 ▲ Triangulation point (in meter)
- • Elevation point (in meter)

Table (1): Modal composition of the examined younger granites.

Sample Number	Rock Unit	Felsic Minerals			Bio.	Mus.	Accessory Minerals	Q	A	P
		Qz	K-fel.	Plag.						
70	Alkali feldspar granite	33.4	61.6	3.2	0.9	0.0	0.9	34.5	62.0	3.5
71		38.6	56.9	3.1	0.7	0.4	0.3	39.0	57.5	3.5
72		31.4	63.4	3.6	0.8	0.2	0.6	32.0	64.0	4.0
73		30.1	64.8	3.0	1.0	0.3	0.8	31.0	65.5	3.5
74		28.7	67.5	2.2	0.9	0.0	0.7	29.5	68.0	2.5
75		26.7	66.6	4.9	0.6	0.3	0.9	27.5	67.0	5.5
Average		31.6	63.6	3.1	0.8	0.2	0.7	32.3	64.0	3.7
60	Syenogranite	33.9	46.9	16.6	1.3	0.4	0.9	35.0	48.0	17.0
61		43.9	42.4	11.3	0.4	0.0	2.0	45.0	43.0	12.0
62		41.5	39.1	17.4	0.7	0.0	1.3	42.0	40.0	18.0
63		37.2	45.3	15.0	0.6	0.0	1.9	38.0	46.0	16.0
64		45.3	38.6	14.5	0.2	0.5	0.9	46.0	39.0	15.0
65		36.2	45.3	16.3	0.7	0.0	1.5	37.0	46.0	17.0
66		47.4	36.3	14.6	0.3	0.0	1.4	48.0	37.0	15.0
67		41.3	42.2	14.7	0.7	0.3	0.8	42.0	43.0	15.0
Average		40.6	42.1	15.1	0.6	0.1	1.3	41.6	42.8	15.6
50	Monzogranite	36.1	24.2	37.2	1.4	0.3	0.8	37.0	25.0	38.0
51		40.0	24.9	32.1	1.2	0.7	1.1	41.0	26.0	33.0
52		38.9	27.7	29.8	1.3	0.0	2.3	40.0	29.0	31.0
53		35.1	31.4	31.1	1.8	0.2	0.4	36.0	32.0	32.0
54		32.2	25.3	40.4	1.4	0.0	0.7	33.0	26.0	41.0
55		29.3	35.1	33.5	0.9	0.0	1.2	30.0	36.0	34.0
56		41.6	23.0	31.2	2.4	0.0	0.9	43.0	25.0	32.0
57		33.4	31.9	32.0	2.1	0.0	0.6	34.0	33.0	33.0
Average		35.9	27.9	33.4	1.6	0.2	1.0	36.8	29.0	34.2

Qz = quartz. Mus. = muscovite. Q = quartz content.
K-fel. = potash feldspar. Bio. = biotite. A = potash feldspar content.
Plag. = plagioclase. P = plagioclase content.
* Note: All values are in volume percent.

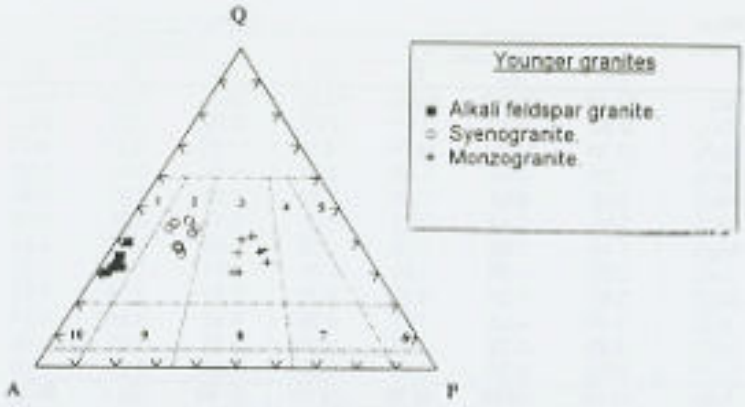

Fig. (2): QAP diagram of the studied younger granites, after Streckeisen (1976).
1 = Alkali granite, 2 = Syenogranite, 3 = Monzogranite, 4 = Granodiorite, 5 = Tonalite, 6 = Quartz diorite,7 = Quartz monzodiorite, 8 = Quartz monzonite, 9 = Quartz syenite and 10 = Quartz alkali-feldspar syenite.

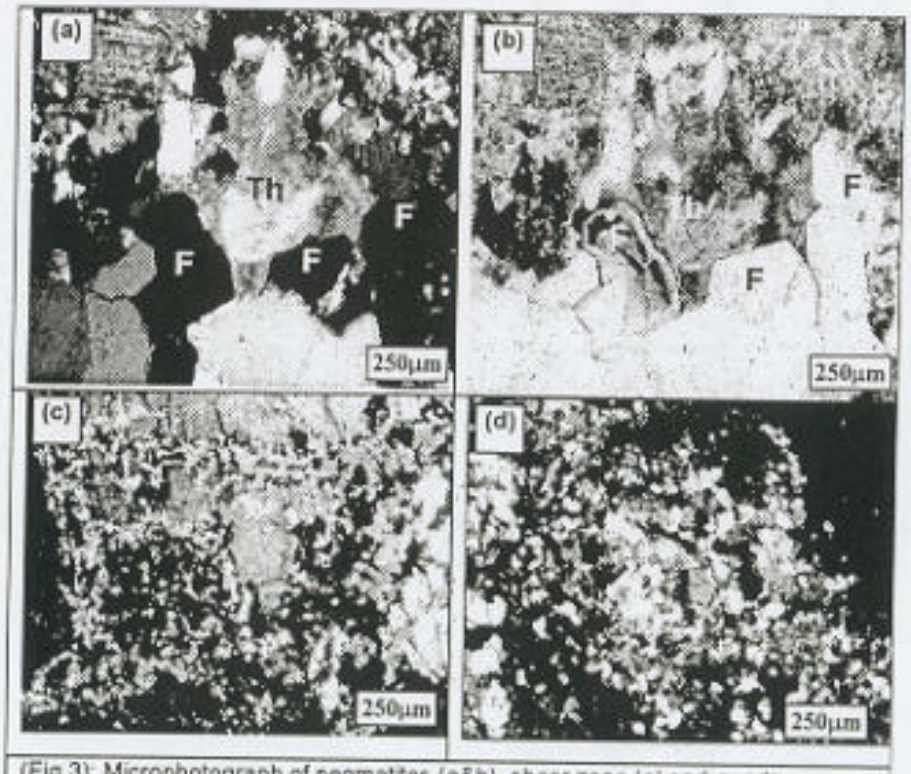

(Fig.3): Microphotograph of pegmatites (a&b), shear zone (c) and quartz veins (d). F = Fluorite and Th = Thorite.
(a,c,d) Crossed Nicol, (b) Polarized Light.

Table (2): Chemical analyses of the studied younger granites.

Major oxides	Younger granites									
	Monzogranite				Syenogranite			Alkali feldspar granite		
	51	52	53	54	65	61	62	70	71	72
SiO_2	72.19	71.09	69.30	68.61	73.11	75.35	74.09	75.80	76.70	74.96
TiO_2	0.34	0.43	0.38	0.31	0.25	0.29	0.23	0.15	0.17	0.19
Al_2O_3	13.34	13.24	14.01	14.64	13.65	13.23	13.60	13.05	12.55	12.35
Fe_2O_3	1.08	1.49	2.06	2.41	1.19	0.44	0.61	0.87	0.63	0.78
FeO	0.48	0.87	1.28	1.35	0.30	0.20	0.59	0.36	0.25	0.61
MnO	0.08	0.10	0.08	0.06	0.04	0.05	0.10	0.05	0.04	0.06
MgO	1.12	1.60	1.79	1.59	0.88	0.70	0.93	0.39	0.30	0.49
CaO	2.25	1.96	1.84	1.95	1.01	1.13	0.97	0.78	0.86	1.00
Na_2O	3.91	4.24	4.20	4.20	3.79	3.74	3.67	3.84	3.91	3.89
K_2O	4.40	4.36	4.51	4.29	4.95	4.56	4.34	4.34	4.41	4.36
P_2O_5	0.20	0.26	0.06	0.19	0.16	0.09	0.08	0.11	0.12	0.12
L.O.I	0.59	0.31	0.45	0.39	0.66	0.26	0.76	0.46	0.56	0.91
Total	99.98	99.99	99.96	99.99	99.99	100.4	99.99	100.2	100.0	99.74
Trace elements (in ppm)										
Rb	105	113	131	101	135	123	131	٩	10	7
Sr	83	94	91	84	57	63	54	6	9	7
Ba	410	422	417	444	265	278	286	11	8	10
Zr	191	226	221	195	210	231	223	9	14	6
Y	46	69	46	55	75	45	51	3	3	2
Nb	35	30	24	27	44	27	25	<٢	<٢	<٢
Zn	52	66	46	53	50	73	65	<٢	<٢	٢
Pb	28	25	24	28	31	25	23	<2	<2	2
V	27	29	28	30	18	28	26	<٢	٢	4
Cr	79	60	75	64	59	36	30	٢	<2	2
Ni	4	3	3	2	7	5	5	<٢	٥	٢
Co	6	4	7	5	9	4	4	<٢	3	٢
Ga	22	23	20	22	25	18	21	2	<2	3
Cu	16	11	15	14	3	6	2	<٢	<٢	<2

Table (3): Chemical analyses of the studied pegmatites, shear zone and quartz veins.

Major oxides	Pegmatites				Shear zone (Altered rock)			Quartz veins (Mineralized)		
	1	2	3	4	5	6	7	8	9	10
SiO_2	69.5	70.4	70.4	68.2	41.53	36.57	44.80	69.75	69.34	71.20
TiO_2	0.32	0.33	0.34	0.21	0.53	0.22	0.36	0.13	0.19	0.11
Al_2O_3	15.08	15.6	13.91	13.91	7.15	6.77	7.6	1.15	1.21	0.80
Fe_2O_3	0.9	0.87	1.0	1.4	37.56	41.0	33.4	24.53	26.03	24.94
FeO	0.34	0.36	0.55	0.65	1.4	1.25	2.12	2.45	1.90	1.67
MnO	0.03	0.05	0.04	0.4	0.16	0.18	0.19	0.06	0.03	0.05
MgO	0.9	0.31	0.8	1.2	1.2	1.0	1.3	0.5	0.23	0.14
CaO	2.83	2.52	2.24	3.92	1.42	1.2	2.01	0.42	0.24	0.19
Na_2O	4.25	4.52	4.53	2.92	0.92	0.45	0.75	0.92	0.10	0.57
K_2O	5.64	4.62	4.32	5.34	3.02	3.73	2.62	0.02	0.75	0.48
P_2O_5	0.02	0.02	0.09	0.07	2.04	2.21	1.31	0.04	0.16	0.09
L.O.I	0.41	0.44	0.81	1.78	3.0	3.32	3.52	1.00	0.82	0.75
Total	100.31	100.04	99.04	99.64	99.93	99.90	99.98	99.97	100.0	99.99
Trace elements (in ppm)										
Rb	396	248	229	358	53	65	59	٩	10	7
Sr	47	30	43	55	48	37	42	6	9	7
Ba	262	345	287	318	557	499	512	11	8	10
Zr	731	618	675	752	21	49	26	9	14	6
Y	562	572	529	593	13	11	13	3	3	2
Nb	334	371	427	433	<2	3	<2	<٢	<٢	<٢
Zn	36	103	52	55	69	54	73	<٢	<٢	٢
Pb	23	28	16	20	29	33	30	<2	<2	2
V	<2	3	2	2	4	3	4	<٢	٢	4
Cr	28	37	29	30	32	27	29	٢	<2	2
Ni	14	7	6	15	7	8	8	<٢	٥	٢
Co	3	4	3	4	48	44	51	<٢	3	٢
Ga	29	34	20	28	14	12	18	2	<2	3
Cu	18	14	11	12	3692	3851	3655	<٢	<٢	<2

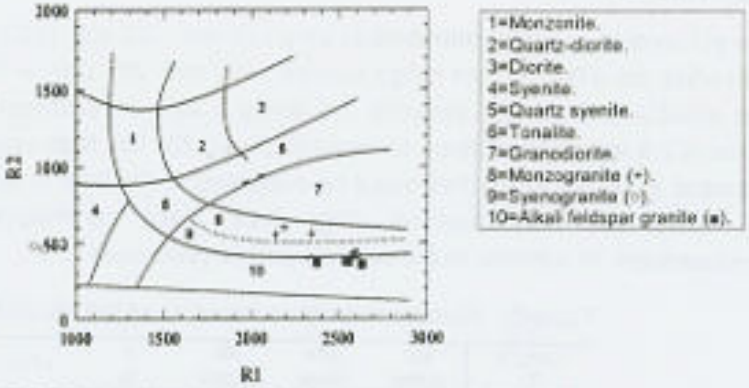

fig. (4): R1-R2 plot for the studied younger granites, after De La Roche/ et al. (1980).
$R_1 = 4\ SiO_2 - 11(Na_2O+K_2O) - 2(FeO^t+TiO_2)$.
$R_2 = 6CaO + MgO + Al_2O_3$.

RADIOMETRIC MEASUREMENTS

Equilibrium states of uranium were calculated using the D-factor (eU / Ra) (Hansink, 1976). If the D-factor equals more than one, this indicates addition of uranium and if equals less than one, this indicates migration of uranium.

Younger granites

The younger granites have wide variation in both eU and eTh contents (Table 4). The eU contents vary between 3 and 14 ppm with an average of 7.5 ppm while eTh contents range between 11 and 40 ppm with an average of 17.5 ppm. The average eTh/eU ratios is 2.8 and the D-factor is 0.9 indicating migration of uranium.

Table (4): Radiometric measurements of the studied younger granites.

Sample No.	Rock type	eU (ppm)	eTh (ppm)	Ra (ppm)	K %	eTh/eU	eU/Ra
70	Alkali feldspar granite	4	11	9	3.89	2.8	0.4
71		12	19	13	4.04	1.6	0.9
72		4	18	4	3.38	4.5	1.0
73		4	21	9	4.43	5.3	0.4
74		5	18	4	3.51	3.6	1.3
75		4	11	4	3.77	2.8	1.0
60	Syenogranite	7	11	8	3.11	1.6	0.9
61		14	40	13	3.22	2.9	1.1
62		11	40	12	3.31	3.6	0.9
63		4	11	5	2.53	2.8	0.8
64		4	14	9	2.80	3.5	0.4
65		13	14	11	2.77	1.1	1.2
66		14	19	15	3.44	1.4	0.9
67		11	18	12	4.5	1.6	0.9
50	Monzogranite	12	14	13	3.89	1.2	0.9
51		9	22	9	2.96	2.4	1.0
52		7	20	8	3.05	2.9	0.9
53		5	11	7	2.79	2.2	0.7
54		3	14	5	2.68	4.7	0.6
55		6	15	10	2.84	2.5	0.6
56		6	11	7	2.28	1.8	0.9
57		6	13	6	2.59	2.2	1.0
Average		7.5	17.5	8.8	3.3	2.8	0.9

Two radioactive anomalies are recorded in the studied area, the first one located in the pegmatites, while, the other is found within the shear zone.

Pegmatite bodies

The eU contents in pegmatite bodies vary between 123 and 182 ppm with an average of 157 ppm while the eTh contents range between 152 and 281 ppm with an average of 242.3 ppm. The eTh/eU ratios range between 0.9 and 2.3 with an average of 1.6 and the average D-factor is 2.9 indicates addition of uranium (Table 5). The high values of uranium and thorium recorded in some pegmatites could be explained in the light of syngenetic concept, in which, the radioactive mineralization stage took place contemporaneously with pegmatite emplacement. In addition to the post magmatic processes.

Table(5): Radiometric measurements of the studied pegmatites.

Sample No.	*eU (ppm)*	*eTh (ppm)*	*Ra (ppm)*	*K %*	*eTh/eU*	*eU/Ra*
1	161	251	37	3.33	1.6	4.4
2	123	258	71	3.40	2.3	1.7
3	182	281	101	3.89	1.5	1.8
4	162	152	46	4.45	0.9	3.5
Average	157	242.3	63.8	3.80	1.6	2.9

Shear zone

The shear zone displays eU contents range between 52 and 79 ppm with an average of 65.3 ppm while the eTh contents vary between 27 and 39 ppm with an average of 31.7 ppm. The eTh/eU ratios range from 0.4 to 0.8 with an average of 0.5 and the D-factor is 2.13 indicates addition of uranium (Table 6). The probable origin of the radioactive anomalies recorded in the shear zone could be attributed to the epigenetic concept, in which, the secondary ascending hydrothermal solutions carry out the radioactive minerals to deposit mainly along fractures, faults and shear zones. In addition to leaching concept, in which, the uranium has been leached from other surrounding rocks, transported by means of circulating water and finally deposited in the shear zone. Attawiya (1983) mentioned that uranium could be released from the granite itself by dissolution of accessory uranium bearing minerals and then re–deposited in shear zones by percolating solution. The field evidence supports this concept where, the radioactivity increased along fractures, faults and shear zones, and the radioactive intensity increases with depth. Generally, the presence of fluorite reveals the hydrothermal origin of the mineralization (Sarcia, 1958).

Table (6): Radiometric measurements of the studied shear zone.

Sample No.	*eU (ppm)*	*eTh (ppm)*	*Ra (ppm)*	*K %*	*eTh/eU*	*eU/Ra*
5	65	27	22	2.27	0.4	2.95
6	79	29	32	1.72	0.4	2.5
7	52	39	55	1.97	0.8	0.95
Average	65.3	31.7	36.3	2.00	0.5	2.13

MINERALOGICAL INVESTIGATIONS

1. Pegmatites

Apatite, bastnasite, betafite, brannerite, cassiterite, columbite, fluorite, goethite, lanarkite, lepidocrocite, malachite, parisite, pisckite, polycrase, thalenite, thorite, xenotime, yttrocrasite, zircon and metamict zircon minerals were detected in pegmatites. The XRD of some concerned minerals are shown in table (7). The BSE images of zircon are shown in figs. (5&6) and the EDX of most investigated minerals are shown in figs. (7&8).

Table (7): X-ray diffractogram of some picked minerals in the studied pegmatites.

Sample (a)		Zircon (6-0266)*		Xenotime (9-377)*	
dA	I/I.	dA	I/I.	dA	I/I.
4.55	33			4.54	25
4.48	46	4.43	45		
3.45	35			3.443	100
3.34	100	3.30	100		
2.70	18			2.744	9
2.56	43			2.558	60
2.54	49	2.518	45		
2.37	9	2.336	10		
2.25	6			2.265	9
2.10	18	2.066	20		
1.92	17			1.927	13
1.77	20	1.751	12	1.762	45
1.73	36	1.712	40	1.721	17
1.67	13	1.651	14	1.681	7
1.59	4	1.547	4	1.608	5

* ASTM card.

Table (7): Cont.

Sample (b)		Cassiterite (5-0467)*		Lanarkite (12-775)*	
dA	I/I.	dA	I/I.	dA	I/I.
3.34	51	3.351	100	3.33	100
3.15	100			3.16	10
2.94	56			2.95	100
2.82	13			2.84	30
2.62	10	2.644	81		
2.01	6			2.05	40
1.93	21			1.91	15
1.77	5	1.765	63	1.76	10
1.70	7	1.675	63	1.72	10
1.56	7	1.593	8	1.57	20
1.52	6	1.498	13	1.51	5
1.42	2	1.415	15	1.435	15

* ASTM card.

Table (7): Cont.

Sample (c)		Malachite (10-399)*	
dA	I/I.	dA	I/I.
5.97	72	5.993	55
5.04	57	5.055	75
3.69	41	3.693	85
2.85	100	2.857	100
2.77	31	2.778	45
2.52	29	2.520	55
2.18	3	2.186	20
1.68	5	1.678	14

* ASTM card.

Table (7): Cont.

Sample (d)		Fluorite (4-864)*	
dA	I/I.	dA	I/I.
3.16	89	3.16	89
1.93	25	1.93	100
1.64	9	1.64	9

* ASTM card.

Table (7): Cont..

Sample (e)		Bastnasite (11-340)*	
dA	I/I.	dA	I/I.
4.88	7	4.88	40
3.50	9	3.564	70
2.88	6	2.879	100
2.45	5	2.445	9
2.02	8	2.016	40
1.90	6	1.898	40
1.51	2	1.481	9

* ASTM card.

Table (7): Cont.

Sample (f)		Goethite (17-537)*		Lepidocrocite (8-98)*	
dA	I/I.	dA	I/I.	dA	I/I.
6.29	41			6.28	100
5.01	17	5.00	20		
4.21	100	4.21	100		
3.30	14			3.29	90
2.71	41	2.69	80		
2.59	23	2.57	20		
2.52	19	2.51	10		
2.46	62	2.44	70	2.47	80
2.25	11	2.25	20		
2.19	23	2.18	40		
2.00	3	2.00	10		
1.94	8	1.92	10	1.937	70
1.85	4			1.848	20
1.80	7	1.803	20		
1.72	27	1.719	50	1.732	40
1.70	15	1.689	20		
1.61	4	1.602	20		
1.57	19	1.563	30	1.566	20

* ASTM card.

Fig. (5):BSE image show zircon grain.

Fig. (6):BSE image show twinning of zircon grains.

2. Shear zone

Several minerals were recorded in shear zone as bismite, fluorite, goethite, hematite, ilmenite, lanarkite, lepidocrocite, malachite, phlogopite, thorite and uranothorite. The XRD of some minerals are shown in table (8). The EDX of most investigated minerals are shown in fig. (9). Milovesky and Kononov (1985) concluded that, in oxidation zone and at the expense of the destruction of chalcopyrite the following minerals are formed: native copper, chalcocite, covellite, cuprite, malachite, azurite, etc...

3. Quartz veins

Goethite and hematite are recorded in quartz veins. The XRD analysis of hematite and goethite is shown in table (9). The EDX of goethite is shown in fig.(10).

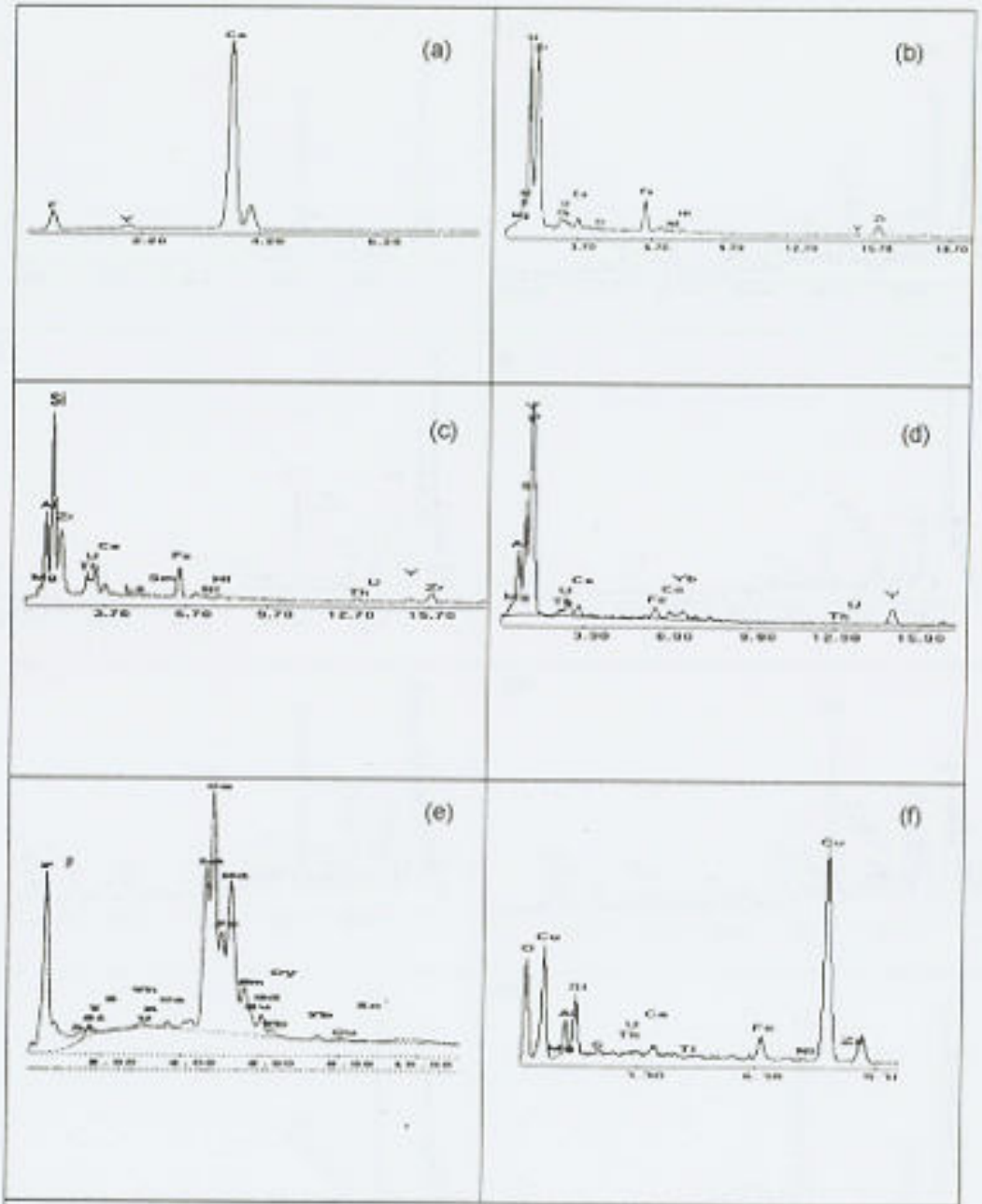

Fig. (7): EDX show: (a) Fluorite, (b) Zircon, (c) Metamict zircon, (d) Xenotime, (e) Parisite, (f) Malachite , in pegmatites

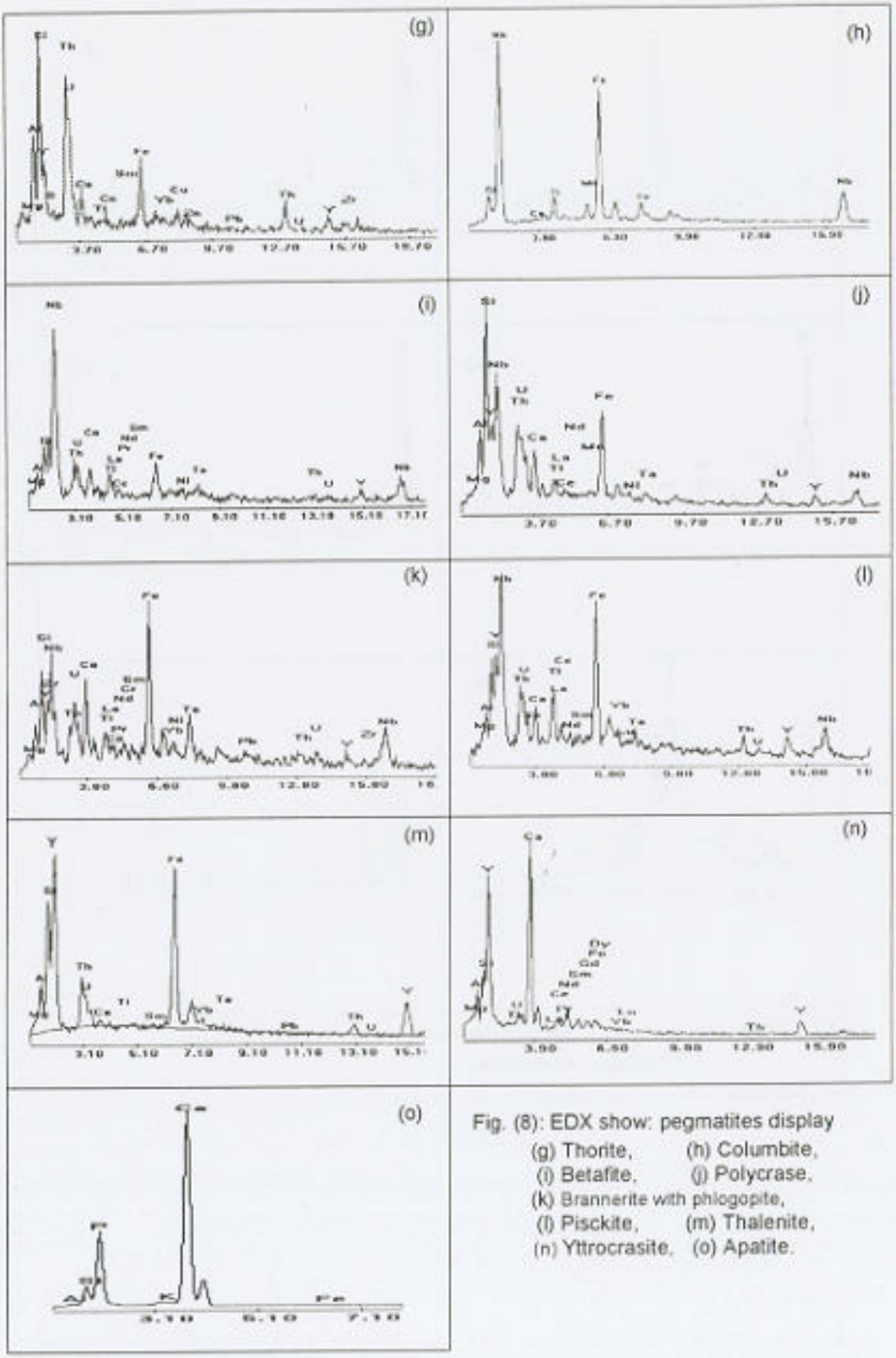

Fig. (8): EDX show: pegmatites display
(g) Thorite, (h) Columbite,
(i) Betafite, (j) Polycrase,
(k) Brannerite with phlogopite,
(l) Pisckite, (m) Thalenite,
(n) Yttrocrasite, (o) Apatite.

Table (8): X-ray diffractogram of some picked minerals in the studied shear zone.

Sample (a)		Goethite (17-537)*		Lepidocrocite (8-98)*		Hematite (13-534)*		Lanarkite (12-775)*	
dA	I/I.	dA	I/I.	dA	I/I.	dA	I/I.	dA	I/I.
6.25	18			6.26	100			6.2	20
4.98	13	4.98	10						
4.18	100	4.18	100						
3.68	23					3.66	25		
3.68	12							3.67	60
3.34	27			3.29	90			3.33	100
2.94	12							2.95	100
2.70	100					2.69	100		
2.70	91	2.69	30						
2.58	22	2.58	8						
2.52	44					2.51	50		
2.52	43	2.52	4						
2.45	88	2.452	25	2.47	80			2.42	70
2.29	5					2.265	2		
2.25	24	2.252	10					2.26	12
2.21	23							2.22	10
2.21	21					2.201	30		
2.19	28	2.192	20						
2.01	6	2.001	2					2.05	40
1.93	9	1.92	6	1.937	70			1.91	15
1.84	21					1.383	40		
1.84	18			1.848	20			1.84	50
1.80	6	1.799	8						
1.72	33	1.721	20	1.732	40			1.72	10
1.69	46					1.69	60		
1.69	32	1.694	10					1.67	15
1.60	8	1.606	6						
1.56	22	1.564	16	1.566	20			1.57	20
1.51	16	1.509	10	1.524	40			1.51	5
1.48	8	1.467	4					1.48	20
1.45	22	1.453	10	1.449	10			1.445	20

* ASTM card.

Table (8): Cont.

Sample (b)		Fluorite (4-864)*	
dA	I/I.	dA	I/I.
3.15	26	3.153	94
1.93	17	1.931	100
1.64	7	1.647	35

* ASTM card.

Table (8): Cont.

Sample (c)		Malachite (10-399)*	
dA	I/I.	dA	I/I.
5.93	59	5.993	55
5.04	42	5.055	75
3.70	56	3.693	85
3.70	56	2.857	100
3.70	56	2.778	45
2.51	63	2.520	55

* ASTM card

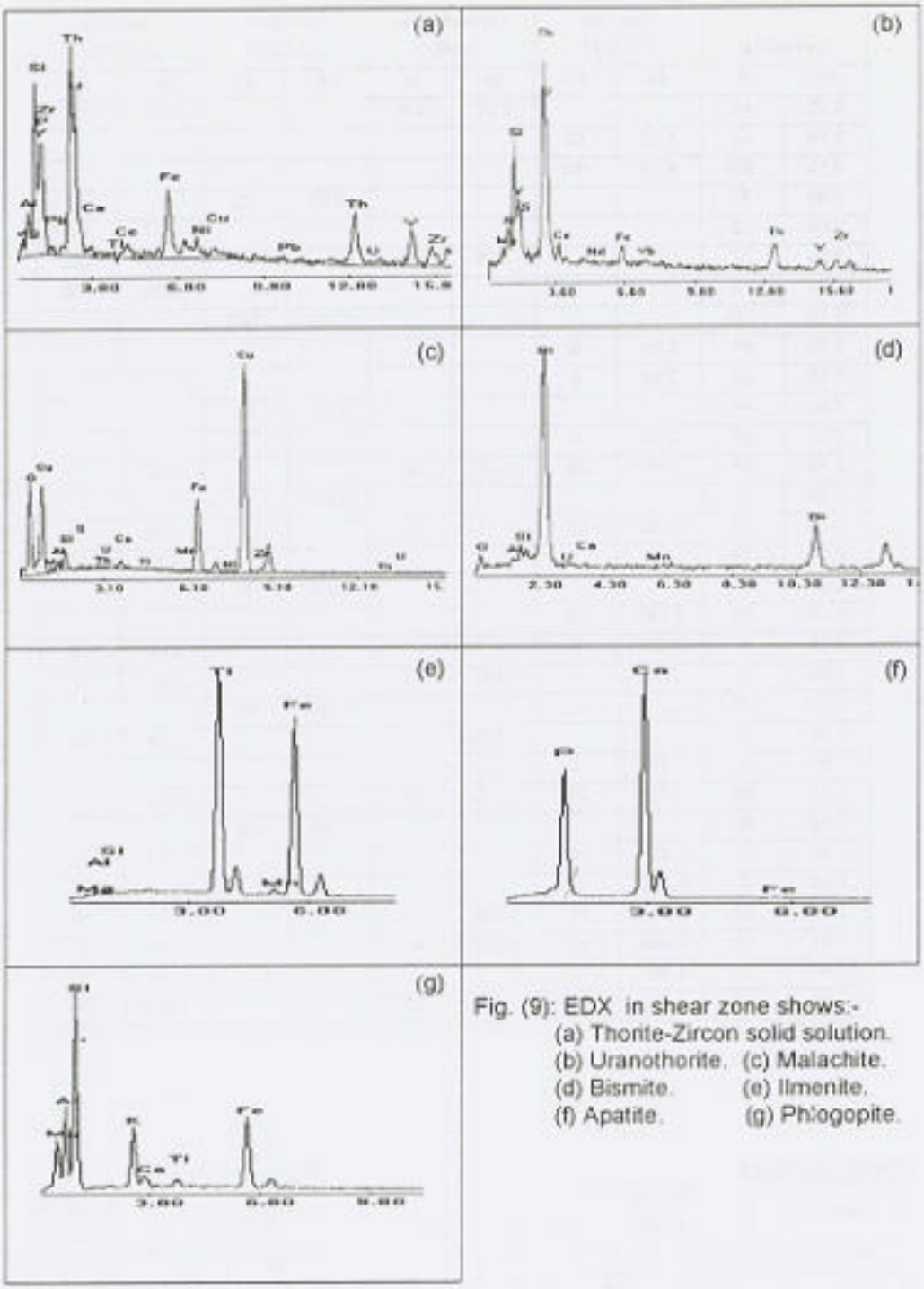

Fig. (9): EDX in shear zone shows:-
(a) Thorite-Zircon solid solution.
(b) Uranothorite. (c) Malachite.
(d) Bismite. (e) Ilmenite.
(f) Apatite. (g) Phlogopite.

Table (9): X-ray diffractogram of some picked minerals in the studied quartz veins.

Sample (a)		Hematite (13-534)*		Goethite (17-537)*	
dA	I/I.	dA	I/I.	dA	I/I.
4.96	8			4.98	10
4.18	8			4.18	100
3.68	16	3.66	25		
3.35	9			3.38	10
2.70	100	2.69	100		
2.70	67			2.69	30
2.57	18			2.58	8
2.52	33	2.51	50		
2.52	20			2.52	4
2.45	100			2.42	25
2.28	5	2.282	2		
2.26	28			2.252	10
2.21	25	2.201	30		
2.18	32			2.192	20
1.93	8			1.92	6
1.84	30	1.838	40		
1.80	17			1.799	8
1.72	50			1.721	20
1.70	40			1.694	10
1.69	38	1.69	60		
1.60	9	1.596	16	1.606	6
1.56	29			1.564	16
1.49	21	1.484	35	1.509	10
1.45	18	1.452	35		
1.45	28			1.453	10

*ASTM card.

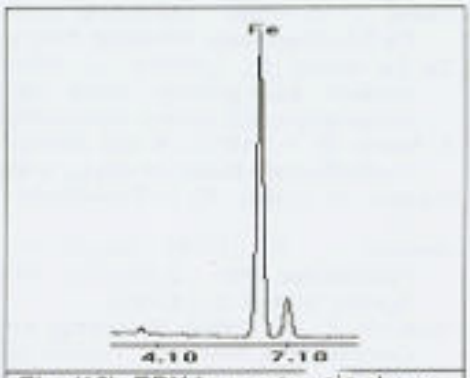

Fig. (10): EDX in quartz vein shows goethite.

CONCLUSIONS

The chemical analyses of the studied pegmatites, shear zone, quartz veins and their host rock (younger granites) revealed that the younger granites display normal contents of major oxides and trace elements. Pegmatites attain high concentrations of Zr, Y, Nb, Rb and Ba. Shear zone contains high concentrations of Fe_2O_3, Cu and Ba, whereas, quartz veins exhibits high concentration of Fe_2O_3.Two radioactive anomalies are recorded in younger granites of the studied area. The first is located in pegmatite bodies while the other was found within the Shear zone. The eU contents in pegmatite bodies vary between 123and 182 ppm with an average of 157 ppm while the eTh contents range between 152 and 281ppm with an average of 242.3 ppm.The shear zone displays high eU contents range between 52 and 79 ppm with an average of 65.3 ppm while the eTh contents vary between 27 and 39 ppm with an average of 31.7 ppm. Apatite, bastnasite, betafite, brannerite, cassiterite, columbite, fluorite, goethite, lanarkite, lepidocrocite, malachite, parisite, pisckite, polycrase, thalenite, thorite, xenotime, yttrocrasite, zircon and metamict zircon were detected in pegmatites. In shear zone, bismite, fluorite, goethite, hematite, ilmenite, lanarkite, lepidocrocite, malachite, phlogopite, thorite and uranothorite were recorded. Goethite and hematite were recorded in the concerned quartz veins. Thorite is isomorphic with zircon and it is evident that, a large part of thorium is

incorporated in the zircon structure (Rankama and Sahama, 1955). Xenotime was occurs as grains as well as inclusion in zircon grains. Heinrich (1958) indicated that, larger zircon grains are included among them apatite, monazite, xenotime, rutile, hematite, magnetite, ilmenite, cassiterite, biotite, tourmaline and quartz, also, he concluded that, in thalenite considerable Th (up to 12% ThO_2) may substitute for Y; U is usually minor, up to about 4% UO_3, but commonly less than 1%.

REFERENCES

Akaad, M. K. and El-Ramly, M. F. (1960): Geological history and classification of the basement rocks of Central Eastern Desert, Egypt. Geol. Surv. Egypt. No. 9, 24 p.

Attawiya, M. Y. (1983): Mineralogical study of El-Erediya-1 uranium occurrence, Eastern Desert, Egypt. Arab. J. Nucl. Sci. Tech., (2) 16, p. 221-234.

Bentor, Y. K. (1985): The crustal evolution of the Arabo-Nubian Massif with special reference to the Sinai Peninsula. Precamb. Res. v. 28, p. 1-74.

De La Roche, H., Leterrier, J., Grandclaude, P. and Marchal, M. (1980): A classification of volcanic and plutonic rocks using R1-R2 diagram and major element analyses; its relationships with current nomenclature Chem. Geol., v. 29, p. 183-210.

El-Ramly, M. F. (1972): A new geological map for the basement rocks in the Eastern and South-Western Desert of Egypt, scale 1: 1000.000. Annal. Geol. Surv. Egypt, v. 2, p. 1-18.

Halpern, M. (1980): Rb-Sr Pan-African isochron ages of Sinai igneous rocks. Geology, v. 8, p 48-50.

Hansink, J. P. (1976): Equilibrium analysis of sandstone rolls front uranium deposits. Proceedings Inter, Symposium on exploration of uranium deposits. Int. Atomic Energy of Agency, Vienna, p. 683-693.

Heinrich, E. W. (1958): Mineralogy and geology of radioactive raw materials. Mc-Graw Hill Book Company, Inc. New York, Toronto, London. 654 p.

Hussein, A. A., Ali, M. M. and El Ramly, M. F. (1982): A proposed new classification of the granites of Egypt. J. Volc. and Geotherm, Res., v. 14, p. 187-198.

Ibrahim, M. A. A. (1996): Uranium mineralization associated with copper occurrences in Sinai, Egypt. Ph. D. Thesis, Ain Shams Univ., 202 p.

Milovsky, A. V. and Kononov, O. V. (1985): Mineralogy. Mir Publishers Moscow. 320 p.

Rankama, K. and Sahama, T. G. (1955): Geochemistry. Chicago Univ. Press, Chicago, 37 p.

Sarcia J.A., (1958): The uraniferous province of northern Limousin and its three principal deposits, Peaceful Uses of atomic Energy, IA. EA. Conf., 2.

Stern, R. J., Gottfried, D. and Hedge, C. E. (1984): Late Precambrian rifting and crustal evolution of the Northeastern Desert of Egypt. Geology, v. 12, p.168-172.

Streckeisen, A. (1976): To each plutonic rocks its proper name. Earth Sci. Rev., v. 12, p. 1-33.

دراسات اشعاعية و معدنية لصخور الجرانيت الحديث بمنطقة جبل شيخ العرب جنوب سيناء - مصر.

*عبد المنعم محمد عثمان، **إبراهيم القطانى السيد العاصى، **على على عبد الرحمن الموافى،

**صلاح صبحى البلاقصى و **أسامه رياض سلام.

*قسم الجيولوجيا – كلية العلوم – جامعة عين شمس – القاهرة.

**هيئة المواد النووية ص.ب ٥٣٠ المعادى – القاهرة.

أوضحت الدراسة الحقلية بالمنطقة أن صخور الجرانيت الحديث قد قطعت بالبجماتيت، نطاق التكسير و عروق الكوارتز. الدراسة الكيميائية أوضحت أن صخور البجماتيت غنية بعناصر الزركونيم، الايتريم، النوبيوم، الربيديوم و الباريوم و صخور نطاق التكسير غنية بعناصر أكسيد الحديد، النحاس و الباريوم و صخور عروق الكوارتز التى بها تمعدنات غنية بعنصر أكسيد الحديد.

تم دراسة توزيع النشاط الإشعاعي فى صخور الجرانيت الحديث بالمنطقة و قد لوحظ أن هناك شاذات اشعاعيه تتمركز فى البجماتيت الداخلة فى الجرانيت الحديث حيث يصل متوسط محتوى اليورانيوم ١٥٧ جزء فى المليون ومتوسط محتوى الثوريوم ٢٤٢,٣ جزء فى المليون. وكذلك هناك شاذات اشعاعيه تتمركز فى نطاق التكسير المار فى الجرانيت الحديث حيث يصل متوسط محتوى اليورانيوم ٦٥,٣ جزء فى المليون ومتوسط محتوى الثوريوم ٣١,٧ جزء فى المليون.

الدراسة المعدنية للمنطقة أوضحت أن هناك ثلاث تمركزات معدنية و جميعها تقع فى صخور الجرانيت الحديث، تمعدنات فى البجماتيت و تحتوى على بعض معادن أكسيد الحديد، ملاكايت، فلوريت، زيركون، زينوتيم، كولومبيت، بيتافيت، بوليكريس، ثالينايت، برانيرايت، بتروكريسايت، بيسكايت، توريت، باريسايت، باستنسايت، كاسيتيرايت، لانركايت و أنانايت. تمعدنات فى نطاق التكسير وتحتوى على بعض معادن أكسيد الحديد، الملاكيت، فلوريت، توريت، يورانوتوريت، لانركايت، بسمايت و فلوجوبايت. تمعدنات فى عروق الكوارتز وتحتوى على بعض معادن أكسيد الحديد.